Surface Passivation and Positive Band-Edge Shift of p-Si(111) Surfaces Functionalized with Mixed Methyl/ Trifluoromethylphenylacetylene Overlayers

Miguel Cabán-Acevedo,[†] Kimberly M. Papadantonakis, Bruce S. Brunschwig,[‡] Nathan S. Lewis[*,†,‡]

†Division of Chemistry and Chemical Engineering, and ‡Beckman Institute, California Institute of Technology, Pasadena, California 91125, United States

I. Data Analysis.

I.A. Overlayer Thickness. The thickness of the TFMPA overlayer attached to a functionalized silicon surface was calculated based on an exponential attenuation of the XPS signal intensity of the bulk Si 2*p* peak caused by the presence of surface TFMPA moieties. Note that the attenuation of the Si 2*p* signal caused by methyl groups was assumed to be negligible in comparison to that of TFMPA. We validated this assumption by considering the attenuation of the methyl overlayer using a bilayer overlayer model. However, since the TFMPA results using a bilayer overlayer model were found to be similar to that of a single overlayer model, we utilized a single overlayer model as a simple and efficient model to evaluate the thickness of the TFMPA overlayer. In addition, at TFMPA addition temparatues of 80 °C and 90 °C, the methyl C 1*s* signal was too weak to properly quantify, which further validates the assumption that the attenuation caused by methyl groups is negligible in comparison to TFMPA.

Based on the single overlayer-attenuation model, the intensity of surface CF_3 (I_{CF3}) and bulk Si (I_{Si}) species can be described as:

$$\frac{I_{CF3}}{I_{Si}} = \frac{SF_{CF3}}{SF_{Si}} * \frac{\rho_{TFMPA}}{\rho_{Si}} * \frac{(1 - e^{\left[d/\lambda_1 * Cos(\theta)\right]})}{(e^{\left[d/\lambda_2 * Cos(\theta)\right]})} \quad (1)$$

where *SF* is the sensitivity factor of the elemental line ($SF_{F\,1s} = 1$, $SF_{C\,1s} = 0.278$, and $SF_{Si\,2p} = 0.328$), ρ is the density of the material ($\rho_{TFMPA} = 3.0$ g/cm^3 and $\rho_{Si} = 2.3$ g/cm^3), *d* is the thickness of the overlayer, λ is the attenuation length for photoelectrons caused by the overlayer (λ_1 (C 1*s*) = 3.00, λ_1 (F 1*s*) = 2.13, and λ_2 (Si 2*p*) = 3.41), and θ is the photoemission angle with respect to the analyzer. The density of the TFMPA overlayer was assumed to be 3.0 g/cm^3 based on the reported density for hydrocarbon overlayers on a silicon (111) surface.[1] The attenuation length for C 1*s*, F 1*s* and Si 2*p* photoelectrons caused by inelastic scattering within the overlayer was calculated using a NIST standard database.[2] The overlayer thickness (*d*) was calculated by substituting the corresponding XPS peak-area values and parameters in Eq. 1, and then solving the resulting equation to find the value of *d*. Note that the trifluoromethyl group of TFMPA displays two characteristic XPS signals: one in the high-resolution C 1*s* spectrum and another in the F 1*s* spectrum. Therefore, we calculated *d* by substituting I_{CF3} and SF_{CF3} using the corresponding values for both the C 1*s* and the F 1*s* signal of the trifluoromethyl group. The sensitivity factors for C 1*s*, F 1*s*, and Si 2*p* peaks were obtained from the Kratos AXIS Ultra library.

Table S1 shows the XPS peak-areas used as the experimental input parameters in the single overlayer-attenuation model shown in Figure 3f. The experimental F_3:CF_3 ratio was close to ~1 for all TFMPA addition temperatures (T_{TFMPA}), meaning that the F-C (F 1*s*) peak area was ~3 times larger than the CF_3 (C 1*s*) peak area after accounting for differences in sensitivity factor. Thus, the peak-area ratio for F-C (F 1*s*) and CF_3 (C 1*s*) is consistent with the presence of TFMPA on the Si surface for all T_{TFMPA} conditions.

Table S1. XPS peak-area values obtained from the high-resolution spectrum for Si 2*p*, F 1*s*, and C 1*s*. The experimental F_3:CF_3 ratio was obtained by normalizing the peak-areas by the sensitivity factor and dividing the F 1s peak-area by a factor of three.

Sample	Si $2p_{3/2}$	F-C (F 1*s*)	CF_3 (C 1*s*)	C-Si (C 1*s*)	F_3:CF_3 ratio
T_{TFMPA} = 50 °C	3233.20	960.20	66.91	230.90	1.33

T_{TFMPA} = 60 °C	3178.50	1827.60	151.90	230.20	1.11
T_{TFMPA} = 70 °C	2874.90	3595.20	326.20	216.30	1.02
T_{TFMPA} = 80 °C	1775.60	5767.50	471.50	137.90	1.13
T_{TFMPA} = 90 °C	649.90	5745.40	473.70	53.49	1.12

I.B. Surface Recombination Velocity. The transient change in microwave conductivity obtained from time-resolved conductivity measurements was fitted using a single-exponential decay:[3-4]

$A = y_o + e^{-t/\tau}$ (2)

where τ is the charge-carrier lifetime. The surface recombination velocity (S) was then calculated using:[3-4]

$\frac{1}{\tau} = \frac{2S}{d}$ (3)

where d is the thickness of the silicon substrate.

I.C. Barrier Height. The barrier height (Φ) for functionalized *p*-silicon/Hg-drop junctions was obtained two ways: by fitting the current density (J) under forward bias, and by fitting the differential capacitance (C_d) under reverse bias. The current density was fitted using the thermionic emission model for diodes:[5-6]

$J = A^{**}T^2 e^{\frac{q\Phi}{K_BT}}(e^{\frac{qV}{nk_BT}} - 1)$ (4)

where A^{**} is the modified Richardson's constant for Si (32 A cm^{-2} K^{-2}) for *p*-silicon), k_B is the Boltzmann's constant (1.381×10^{-23} J/K), and T is the temperature in Kelvin (296 K). By convention, the forward-bias region of the J-V curves was depicted and analyzed within the first and fourth quadrant. The differencial capacitance was fitted using the Mott-Schottky equation:[6]

$1/C_d^2 = \frac{2}{q\varepsilon_0\varepsilon N_D A_s^2}(V_{FB} + \frac{K_BT}{q} - V)$ (5)

where q is the absolute value of the elementary charge (1.602×10^{-19} C), ε_0 is the vacuum permittivity (8.85×10^{-14} F/cm), ε is the dielectric constant of silicon (11.8), N_A is the acceptor dopant density, A_S is the junction geometric area in cm^2, and V_{FB} is the flat-band potential. From a $1/C_d^2$–V plot we obtained N_A from the slope using the Mott-Schottky relationship. V_{FB} was obtained from the *x*-intercept (V_0):

$V_0 = V_{FB} + \frac{k_BT}{q}$ (6)

and the barrier height was calculated using the equation:[6]

$\Phi = V_{FB} - \frac{k_BT}{q}\ln(\frac{N_A}{N_V})$ (7)

where N_V is the effective density of states for the valence band edge of silicon (1.0×10^{19} cm^{-3}). By convention, the reverse bias region of the $1/C_d^2$–V plot is within the second quadrant, and the obtained V_{FB} is positive for *p*-silicon.

I.D. The Effect of a Thin Insulating Overlayer on the Total Differencial Capacitance. In the presence of a thin isulating overlayer with a voltage-idependent capacitance, the total differencial capacitance can be described using the equation:[7-8]

$1/C_d^2 = 1/C_L^2 + \frac{2}{q\varepsilon_0\varepsilon N_D A_s^2}(V_{FB} + \frac{K_BT}{q} - V)$ (8)

where C_L is the voltage-idependent capacitance of the insulating overlayer. From a $1/C_d^2$–V plot the constant N_A can be obtained from the slope in the same maner as the standard Mott-Schottky equation (Eq. S5). However, the *x*-intercept (V_0) is modified by the thin insulating overlayer capacitance and it can be described by the equation:[7-8]

$V_0 = V_{FB} + \frac{k_BT}{q} - q\varepsilon_0\varepsilon N_D A_s^2/2C_L^2$ (9)

Since the slope of the linear region in a $1/C_d^2$–V plot for a p-type semiconductor is negative, the insulating overlayer term adds to V_{FB} for a positive dipole overlayer and the *x*-intercept is proportional to $V_{FB} + V_L$, where V_L is the shift induces by C_L. Consequetly, *x*-intercept values larger than the band gap of silicon can be obtained under such condititions.

I.E. Effective Solution Potential of Photoelectrochemical Cells. Differences in the concentration of minority scavenger species concentration among redox couples complicate the evaluation of the V_{OC} linearity with solution potential, due the dependence of the quasi-Fermi level for minority carriers on the minority scavenger concentration.[9] To adequately evaluate the V_{OC} dependence with solution potential, we normalized the minority scavenger (oxidized species) concentration to 10 mM for all redox couples by converting the measured cell potential (E (A/A^-)) to an effective cell potential. The effective cell potential for *p*-silicon electrodes (E_{eff} (A/A^-)) was calculated using the equation:[10]

$$E_{eff}(A/A^-) = E(A/A^-) - \frac{k_B T}{q} \ln \frac{[A_{eff}]}{[A]} \quad (10)$$

where $[A_{eff}]$ is the effective 10 mM concentration of oxidized species, and [A] is the solution concentration of oxidized species.

II. Methylation of chlorine-terminated silicon (111) surface using methylzinc chloride.

Methylzinc chloride (CH_3ZnCl) was investigated as a milder methylating agent for the preparation of methyl-terminated silicon (111) surfaces. Figure S1.a shows the transmission infrared spectroscopy (TIRS) results for a representative chlorine-terminated silicon surface after methylation with CH_3ZnCl at a reaction temperature of ~ 179 °C for 48 h. In the TIRS spectrum, we observed a peak at 1257 cm^{-1} after methylation that can be attibuted to the symmetric bend ("umbrella" mode) for methyl groups on a silicon surface ($\nu(CH_3)$).[11] Further characterization of the chemical composition of the surface after methylation was performed using X-ray photoelectron spectroscopy (XPS) measurements. Figure S1.b-e shows the XP survey spectrum and the corresponding high-resolution C 1*s*, Si 2*p* and Cl 2*p* peak spectra for a representative silicon sample after methylation with CH_3ZnCl. In the C 1*s* spectrum, we observed a peak corresponding to methyl carbons covalently bonded to surface silicon atoms at 284 eV (C-Si), which provides direct evidence for the presence of methyl moieties on the silicon surface. Support for the passivation of the surface was obtained from the high-resolution Si 2*p* spectrum since no detectable amount of silicon oxide was found and only a 2*p* doublet ($2p_{3/2}$ and $2p_{1/2}$ peak splitting) corresponding to bulk silicon can be observed. Trace amounts of unreacted Cl-terminated silicon surface species were also observed on the silicon surface due to the presence of a weak 2*p* doublet in the Cl 2*p* spectrum. Assuming that all surface silicon atoms are terminated by methyl groups or chlorine atoms, we calculated the methyl monolayer coverage (θ_{CH3}) using the area of the $C_{C\text{-}Si}$ 1*s* peak and the Cl $2p_{3/2}$ peak. At a reaction temperature of ~ 179 °C and reaction time of 48 h, the methyl covarage was $\theta_{CH3} = 0.99$ ML. We also found that controllable partial methylation can be achieved using CH_3ZnCl by tuning the reaction temperature. Figure S1.F shows the calculated surface methyl fractional coverage at different reaction temperatures with reaction time of 24 h, where we observed a linear change in θ_{CH3} with reaction temperature.

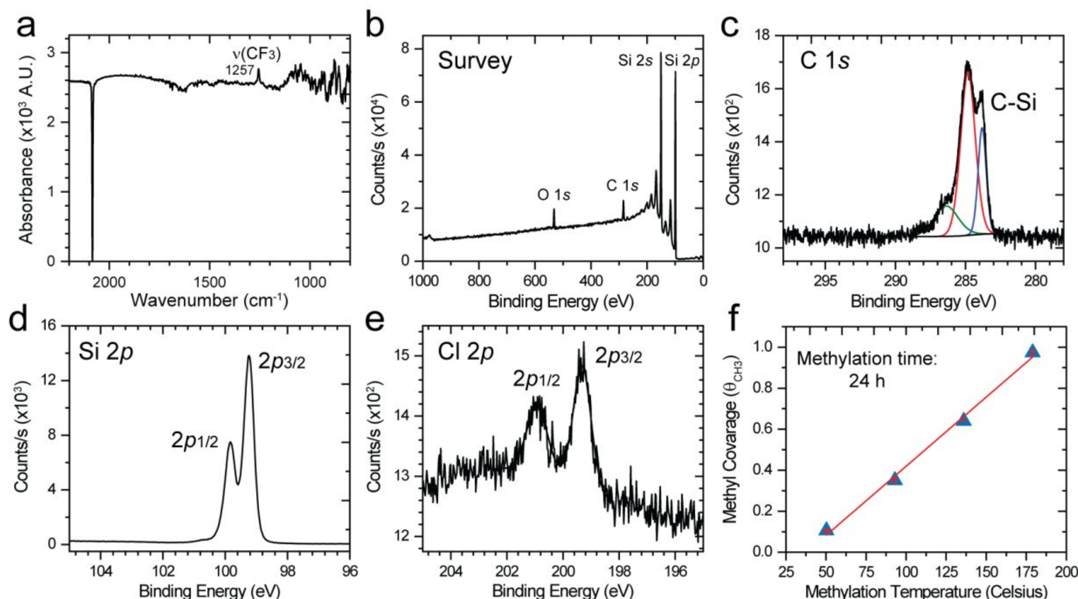

Figure S1. (a) TIRS, (b) XPS survey and high-resolution (c) C 1*s*, (d) Si 2*p*, and (e) Cl 2*p* peak spectra for a representative chlorine-terminated silicon surface after methylation with methylzinc chloride at a reaction temperature of 179 °C for 48 h. Methyl fractional coverage (θ_{CH3}) at different reaction temperatures using methylzinc chloride as the methylating agent and 24 h as the reaction time. Note that the plotted θ_{CH3} values and error bars are the average of two functionalized silicon samples.

III. Synthesis of methyl/TFMPA-terminated silicon surface using partial methylation.

CH_3ZnCl also allows for the synthesis of of mixed 4-trifluoromethylphenylacetelyne (TFMPA) and methyl-terminated silicon (111) by partial methylation followed by nucleophilic addition of TFMPA (Figure S1.a). This alternative reaction step order was enabled by the milder reactivity of CH_3ZnCl (in comparison to CH3MgCl), which allows for controllable partial methylation of chlorine-terminated silicon. Figure S2.b shows the TIRS spectra for a representative methyl/TFMPA-terminated silicon surface prepared by partial methylation at 148 °C for 24 h and subsequent TFMPA addition at 50 °C for 24 h. In the TIRS spectrum we observed peaks at 1329 cm^{-1} and 1253 cm^{-1} which correspond to the vibration of the *para*-trifluoromethyl group of TFMPA moeties ($\nu(CF_3)$) and the symmetric stretch of surface methyl moeties ($\nu(CH_3)$).

Consequently, the TIRS spectrum indicates that methyl/TFMPA-terminated silicon surfaces can be prepared using partial methylation with CH_3ZnCl.

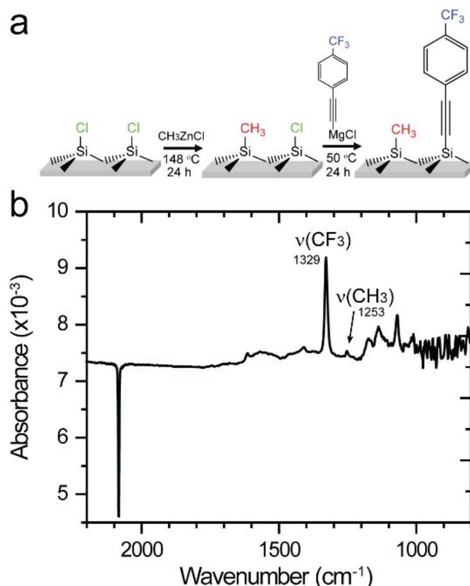

Figure S2. (a) Reaction scheme for the synthesis of methyl/TFMPA-terminated silicon (111) surfaces using partial methylation with methylzinc chloride. (b) TIRS spectra collected at 74° for the mixed methyl/TFMPA-terminated silicon surface prepared using the conditions depicted in panel a.

Figure S3a-e shows the XP survey spectrum and the corresponding high-resolution C 1*s*, Si 2*p* and Cl 2*p* peak spectra for a representative mixed TFMPA/methyl-terminated silicon (111) sample prepared by partial methylation followed by nucleophilic addition of TFMPA. The XPS data for the representative methyl/TFMPA-Si confirmed the presence of both type of moieties on the surface due to the appearance of a C-Si peak and CF_3 in the C 1*s* spectrum (Figure S3b), and a F-C peak in the F 1*s* spectrum (Figure S3d). The Si 2*p* spetrum (Figure S3c) showed only the presence of bulk Si peaks, which indicated that the surface was passivated. A weak 2*p* doublet in the Cl 2*p* spectrum indicated the presence of trace amounts (<0.1 monolayer) of unreacted Cl-terminated silicon species on the silicon surface. Considering that methyl/TFMPA silicon surfaces were sonicated in water prior to XPS measurements, the data are consistent with limitations on the coverage of the Si-Cl surface species due to steric hindrance arising from packing constraints. The presence of only one doublet in the Cl 2*p* spectrum indicated that all residual Cl-terminated surface sites had mutually similar chemical enviorments. Considering that both C-Si and Cl-Si species show a single chemical enviorment the methyl and TFMPA moeties are on average homogeniously distributed on the Si surface. Consequetly, XPS meassurments for methyl/TFMPA-Si indicated that the surface has a distribution of organic moeties similar to TFMPA/methyl-Si samples.

Figure S3f shows the Ln(J)−V characteristics of a p-type methyl/TFMPA-Si surface in contract with Hg. The methyl/TFMPA-Si/Hg junction displayed current rectification (diode behavior) with a barrier height similar to methyl/TFMPA sample prepared at T_{TFMPA} = 60 °C. Therefore, ln(J)−V meassurments also suggest that the distrubition of organic moeties for methyl/TFMPA-Si samples is similar to that of TFMPA/methyl-Si samples.

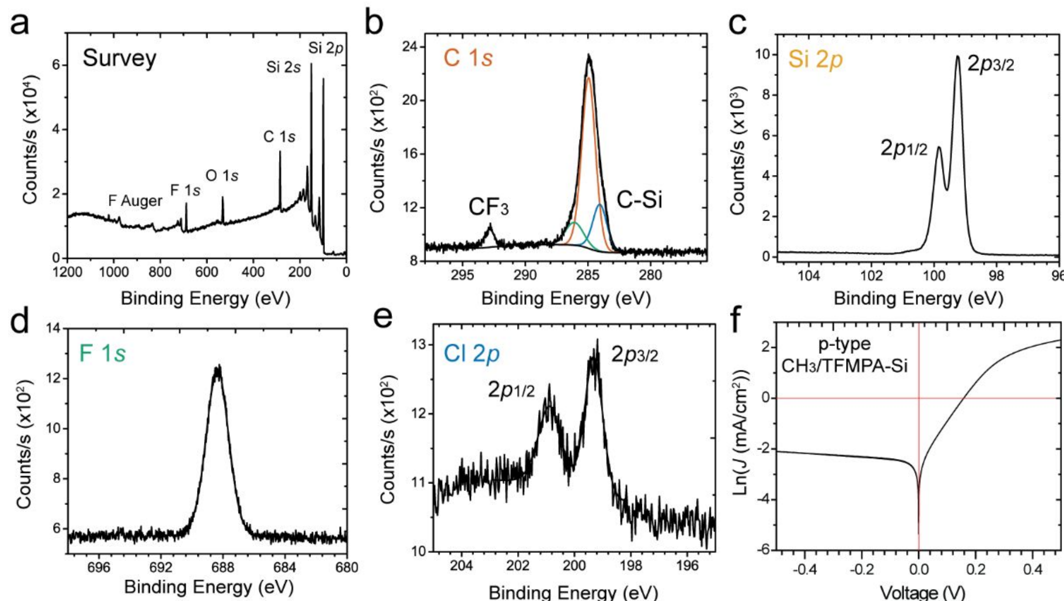

Figure S3. (a) XP survey and corresponding high-resolution spectra for the (b) C 1*s*, (c) Si 2*p*, (d) F 1*s*, and (e) Cl 2*p* regions for a representative mixed methyl/TFMPA-terminated silicon surface. The partial methylation was carried at 148 °C nucleophilic and the subsequent addition of TFMPA was carried at 50 °C. (f) Natural logarithm of the current density vs applied voltage (ln J vs V) for a mixed methyl/TFMPA-terminated p-Si surfaces in contact with a Hg drop.

IV. Comparison of the Bode plot for H-terminated and TFMPA/metyl-terminated p-Si(111) in contact with Hg.

Figure S4 shows that the Bode plot within the reverse bias region and for the AC frequency window of 215 kHz–10 Hz behaved like a simplified Randles circuit of the form of R_1+C_1/R_2. However, within the frequency range of 215 kHz to ~350 Hz, the circuit can be further simplified to just C_1 because the impedance response is purely capacitive. Junction capacitors that are in series (C_2) with the space-charge capacitance (C_{SC}) –such as an organic overlayer capacitance or a double layer capacitance– have the circuit form of R_1+(C_{SC}+C_2)/R_2 or C_{SC}+C_2. Since the series capacitance (C_S) is C_S = 1/C_{SC} + 1/C_2, the circuits R_1+(C_{SC}+C_2)/R_2 or C_{SC}+C_2 are equivalent to the R_1+C_s/R_2 and C_S circuits. Consequently, because of this circuit equivalence the organic overlayer capacitance cannot be separated from the space-charge capacitance, since the junction will display a single effective differential capacitance that will be equal to C_S. When the two capacitors in series have comparable values, the differential capacitance of the junction can display a mixed behavior depending in the difference of this two values. When one of the series capacitors is substantially smaller than the other, the differential capacitance of the junction is dominated by the smaller capacitor.

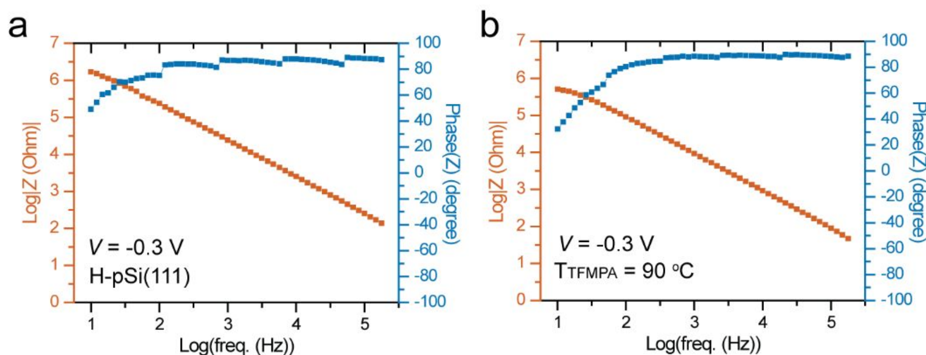

Figure S4. Bode plot Hg junctions with p-type (a) H-Si and TFMPA/methyl-Si prepared at T_{TFMPA} = 90 °C. The Bode plots correspond to an applied DC bias of -0.3 V and AC frequency window of 215 kHz–10 Hz.

V. Mott-Schottky plot for TFMPA/methyl-terminated p-Si electrodes in contact with $(CpCO_2CH_3)_2Co^{+/0}$.

Figure S5 shows the Mott-Schottky plot for TFMPA/methyl-terminated p-Si(111) electrode when using $(CpCO_2CH_3)_2Co^{+/0}$ as redox couple. From linear extrapolation using the Mott-Schottky relationship (Eq. 5) the flat-band

potential (E_{fb}) was obtained from the *x*-intercept and the dopant concentration (N_D) from the slope (Table S2). The value for the solution barrier height (ϕ_{sol}) was then obtained using Eq. 7. Table S2 shows that the E_{fb} value for T_{TFMPA} = 90 °C is positively shifted by 73 mV in comparison to T_{TFMPA} = 60 °C, which indicated an increase in positive surface dipole with an increase in the surface concentration of TFMPA. When T_{TFMPA} = 90 °C was compared with previously reported E_{fb} value for p-type CH_3-Si in contact with $(CpCO_2CH_3)_2Co^{+/0}$ (for similar electrolyte composition), a positive shift was observed of ~140 mV for E_{Fb} and ~157 mV for ϕ_{sol}.[10] Therefore, the Mott-Schottky results for TFMPA/methyl-terminated p-Si when in contact with $(CpCO_2CH_3)_2Co^{+/0}$ were in agreement with the trend observed from V_{OC} and Hg junction meassurments.

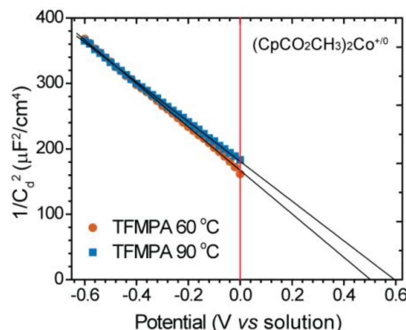

Figure S5. Mott-Schottky (capacitance vs potential; $1/C_d^2$ vs V) plots for T_{TFMPA} = 60 and 90 °C mixed TFMPA/methyl-terminated p-Si(111) electrodes, submerged in acetonitrile electrolytes containing 1.0 M $LiClO_4$ and $(CpCO_2CH_3)_2Co^{+/0}$.

Table S2. Flat-band potentials (E_{fb}) and solution barrier heights (ϕ_{sol}) obtained for the functionalized p-Si(111) electrodes when submerged in acetonitrile electrolyte containing $(CpCO_2CH_3)_2Co^{+/0}$ as redox couple. *The N_D and E_{fb} values for p-type CH_3-Si(111) were obtained from Ref. #10.

p-type Sample	N_D (cm^{-3})	E_{fb} (mV)	ϕ_{sol} (mV)
TFMPA/CH_3-Si T_{TFMPA} = 60 °C	3.5×10^{16}	503	675
TFMPA/CH_3-Si T_{TFMPA} = 90 °C	3.9×10^{16}	576	746
CH_3-Si	7.7×10^{16}*	437*	589*

VI. References.

(1) Webb, L. J.; Nemanick, E. J.; Biteen, J. S.; Knapp, D. W.; Michalak, D. J.; Traub, M. C.; Chan, A. S. Y.; Brunschwig, B. S.; Lewis, N. S. High-Resolution X-Ray Photoelectron Spectroscopic Studies of Alkylated Silicon(111) Surfaces. *J. Phys. Chem. B* **2005**, *109*, 3930–3937.

(2) Powell, C. J. J., A. Nist Electron Inelastic-Mean-Freepath Database, Version 1.2, Srd 71; National Institute of Standards and Technology: Gaithersburg, Md, 2010.

(3) O'Leary, L. E.; Johansson, E.; Brunschwig, B. S.; Lewis, N. S. Synthesis and Characterization of Mixed Methyl/Allyl Monolayers on Si(111). *J. Phys. Chem. B* **2010**, *114*, 14298–14302.

(4) Royea, W. J.; Juang, A.; Lewis, N. S. Preparation of Air-Stable, Low Recombination Velocity Si(111) Surfaces through Alkyl Termination. *Appl. Phys. Lett.* **2000**, *77*, 1988–1990.

(5) Maldonado, S.; Plass, K. E.; Knapp, D.; Lewis, N. S. Electrical Properties of Junctions between Hg and Si(111) Surfaces Functionalized with Short-Chain Alkyls. *J. Phys. Chem. C* **2007**, *111*, 17690–17699.

(6) Sze, S. M. *Physics of Semiconductor Devices*; John Wiley & Sons: New York, 1981.

(7) Cardon, F.; Gomes, W. P. On the Determination of the Flat-Band Potential of a Semiconductor in Contact with a Metal or an Electrolyte from the Mott-Schottky Plot. *J. Phys. D: Appl. Phys.* **1978**, *11*, L63–L67.

(8) Sze, S. M.; Ng, K. K. *Physics of Semiconductor Devices*; John Wiley & Sons, Inc., 2006.

(9) Rosenbluth, M. L.; Lewis, N. S. "Ideal" Behavior of the Open Circuit Voltage of Semiconductor/Liquid Junctions. *J. Phys. Chem.* **1989**, *93*, 3735–3740.

(10) Grimm, R. L.; Bierman, M. J.; O'Leary, L. E.; Strandwitz, N. C.; Brunschwig, B. S.; Lewis, N. S. Comparison of the Photoelectrochemical Behavior of H-Terminated and Methyl-Terminated Si(111) Surfaces in Contact with a Series of One-Electron, Outer-Sphere Redox Couples in Ch_3cn. *J. Phys. Chem. C* **2012**, *116*, 23569–23576.

(11) Webb, L. J.; Rivillon, S.; Michalak, D. J.; Chabal, Y. J.; Lewis, N. S. Transmission Infrared Spectroscopy of Methyl- and Ethyl-Terminated Silicon(111) Surfaces. *J. Phys. Chem. B* **2006**, *110*, 7349–7356.